

High- T_g and Low-Dielectric Epoxy Thermosets Based on a Propargyl Ether-Containing Phosphinated Benzoxazine

Ching Hsuan Lin,¹ Chu Ming Huang,¹ Tung I. Wong,¹ Hou Chien Chang,¹ Tzong Yuan Juang,² Wen Chiung Su³

¹Department of Chemical Engineering, National Chung Hsing University, Taichung, Taiwan

²Department of Applied Chemistry, National Chiayi University, Chiayi, Taiwan

³Department of Chemistry and Chemical Engineering, Chung Shan Institute and Technology, Lungtan, Taoyuan, Taiwan

Correspondence to: C.-H. Lin (E-mail: linch@dragon.nchu.edu.tw) or H.-C Chang (E-mail: hchang@dragon.nchu.edu.tw)

Received 26 November 2013; accepted 23 January 2014; published online 24 February 2014

DOI: 10.1002/pola.27125

ABSTRACT: A propargyl ether-containing benzoxazine (**4**) was prepared from a potassium carbonate-catalyzed nucleophilic substitution of propargyl bromide and a phenolic OH-containing benzoxazine (**3**), which was prepared from 1-(4-hydroxyphenyl)-1-(4-aminophenyl)-1-(6-oxido-6H-dibenz <c,e><1,2> oxaphosphorin-6-yl)ethane (**1**) by a three-step procedure. The curing reactions of (**4**) were monitored by IR and DSC. A reaction mechanism was proposed based on the observation. Benzoxazines (**3**) and (**4**) were applied as epoxy curing agents. The microstructure and the structure-property relationship of the resulting thermosets are discussed. The double-strand structure

in (**4**)-cured epoxy thermosets afforded higher crosslinking density, and led to higher thermal properties. In addition, the (**4**)-cured epoxy thermosets possess half the amount of highly polar hydroxyl groups than those of the (**3**)-cured epoxy thermosets, resulting in a lower dielectric constant, dissipation factor, and water absorption. © 2014 Wiley Periodicals, Inc. *J. Polym. Sci., Part A: Polym. Chem.* **2014**, *52*, 1359–1367

KEYWORDS: benzoxazine; high performance polymer; propargyl; structure-property relations; thermal properties; thermosets

INTRODUCTION Benzoxazines are resins that can be polymerized to phenolic-type thermosets via the thermally activated ring-opening of the oxazine linkage.^{1,2} The epoxy/benzoxazine system has recently been used in the industry of copper clad laminates (CCL) due to the characteristic of higher T_g , better adhesion to glass fiber, and better toughness than the epoxy/phenol novolac system. With the trends of increased circuit density, material with a low dielectric constant is preferred since the signal propagating speed in integrated circuits is inversely proportional to the square root of the dielectric constant, and the signal propagation loss is proportional to the square root of the dielectric constant. Therefore, preparing benzoxazines with the low-dielectric constant is attractive for the CCL industry.

Works on developing low-dielectric polybenzoxazines have been done by various groups. Hamerton et al. prepared a series of bis-benzoxazines from various bisphenols, and found that bisphenol A and hexafluorobisphenol A-based polybenzoxazines exhibit the lowest dielectric constant.³ They also found that the dielectric constant of polybenzoxazines is higher than cured commercial cyanate esters, but comparable

with FR4 epoxy thermosets and bismaleimides. The advantage of incorporating fluoro element in reducing dielectric constant has also been observed by other groups. For example, Su and Chang prepared a low-dielectric polybenzoxazine based on a hexafluorobisphenol A and 4-(trifluoromethyl)aniline-based benzoxazine.⁴ Lin et al. prepared low-dielectric polybenzoxazines from fluorinated diamines and phenol-based benzoxazines.⁵ Velez-Herrera et al. prepared low-dielectric polybenzoxazines from highly fluorinated aliphatic diamines and 4-fluorophenol-based benzoxazines, and fluorinated aromatic diamines and hexafluorobisphenol A-based benzoxazines.⁶ The incorporation of polyhedral oligomeric silsesquioxane (POSS) has been proven to be an effective approach in reducing the dielectric constant.^{7–10} Low-dielectric polybenzoxazines based on octa(maleimido phenyl)silsesquioxane (OMPS), and found that the dielectric decreased from 3.62 for neat polybenzoxazine to 2.42 with 10 wt % OMPS. Tseng and Liu prepared a nanocomposite based on a furan-containing benzoxazine and methyl methacrylate terminated polyhedral oligomeric silsesquioxane (MMA-POSS).¹¹ They found that the dielectric constant was reduced with the content of MMA-POSS. Furthermore, the

Additional Supporting Information may be found in the online version of this article.

© 2014 Wiley Periodicals, Inc.

dielectric constant of the composites can further be reduced via the orientation of POSS into the lamellar structure. Low-dielectric polybenzoxazines can also be prepared from a porous structure. For example, Chang et al. prepared benzoxazine with labile poly(3-caprolactone) linkage.¹² Low-dielectric polybenzoxazine can be achieved after the labile polycaprolactone was decomposed. The introduction of low-polar linkages has also been demonstrated as an effective approach to reduce the dielectric constant. Huang et al. compared three benzoxazines from dicyclopentadiene-phenol adduct, bisphenol A, and 4,4'-biphenol, respectively.^{5,13} They found that polybenzoxazine based on dicyclopentadiene-phenol adduct exhibits the lowest dielectric constant. Recently, Yang and Gu¹⁴ and Zhang et al.¹⁵ prepared low ether-dielectric polybenzoxazines with benzoxazole moieties since polybenzoxazoles are considered to be relatively low-dielectric materials. Hougham et al.^{16,17} reported that the dielectric constant could be reduced by increasing molecule's hydrophobicity, free volume, and by decreasing polarization. Recently, we successfully prepared phosphinated cyanate ester thermoset based on the bulky phosphinate pendant that increased free volume of thermoset.¹⁸

Aryl propargyl ether is known to undergo Claisen type rearrangement to benzopyran with thermal treatment, and subsequently polymerize via the curing of the C=C bond in the benzopyran structure.^{19–26} Preparation of propargyl ether-containing benzoxazine has been reported by Agag and Takeichi,²⁷ Kiskan et al.,²⁸ Chernykh et al.,^{29,30} and Chang et al.³¹ However, no dielectric properties of the propargyl-containing benzoxazine have been discussed in the literature. In this work, we report our strategy in preparing a propargyl ether-containing benzoxazine (**4**) from a nucleophilic substitution of propargyl bromide and a phenolic OH-containing benzoxazine (**3**). Benzoxazines (**3**) and (**4**) were applied as epoxy curing agents. Experimental data show that (**4**)-cured epoxy thermosets show higher thermal properties and a lower dielectric constant than (**3**)-cured epoxy thermosets. The detailed synthesis, curing behavior, and structure-property relationship of the resulting thermosets are reported in this work.

EXPERIMENTAL

Materials

Potassium carbonate, 2-hydroxybenzaldehyde, and propargyl bromide were purchased from Acros; 1-(4-hydroxyphenyl)-1-(4-aminophenyl)-1-(6-oxido-6H-dibenz[*c,e*]⟨1,2⟩oxaphosphorin-6-yl)ethane (**1**) was prepared according to the literature.³² Diglycidyl ether of bisphenol A (DGEBA) with an epoxy equivalent weight (EEW) of 187 g/eq and cresol novolac epoxy (CNE) with an EEW of 200 g/eq were kindly supplied by Chang Chun Plastics, *N,N*-dimethylacetamide (DMAc) was purchased from Tedia and purified by distillation under reduced pressure over calcium hydride (Acros) and stored over molecular sieves. The other solvents used are commercial products and were used without further purification.

Synthesis of (2)

Ten grams (0.012 mol) of (**1**), 2-hydroxybenzaldehyde 3.09 g (0.025 mol), and 50 mL of ethanol were introduced into a 100 mL round-bottom glass flask equipped with a condenser and a magnetic stirrer. The mixture was reacted at room temperature for 12 h. Then, 1.392 g (0.042 mol) NaBH₄ was added. The reaction mixture was stirred at room temperature for 12 h. The mixture was then poured into methanol/water (1/1, V/V). The precipitate was isolated by filtration. After drying, 10.94 g of (**2**) (82% yield) was obtained. HR-MS (FAB+) *m/z*: calcd. for C₃₃H₂₈O₄NP 533.1756; anal., 534.1761 (M+1)⁺.

ELEM ANAL CALCD: C, 74.29%; H, 5.29%; N, 2.63%. Found: C, 72.13%; H, 5.42%, 2.59%. ¹H-NMR (ppm, DMSO-d₆), δ = 1.5 (CH₃), 4.2 (CH₂), 5.9 (NH), 6.4–8.1 (Ar-H), 9.5 (OH).

Synthesis of (3)

Exactly 7.73 g (0.014 mol) of (**2**), 0.696 g (0.023 mol) of paraformaldehyde, and 50 mL of THF were introduced into a 100 mL round-bottom glass flask equipped with a condenser and a magnetic stirrer. The mixture was stirred at room temperature for 4 h, and then further stirred at 50 °C for 12 h. The precipitate was filtered and washed with DI water. After drying, white powder 6.26 g (82% yield) with a melting point of 239 °C (DSC) and an exothermic peak temperature of 245 °C was obtained. HR-MS(FAB+) *m/z*: calcd. for C₃₄H₂₈O₄NP 545.1755; anal., 546.1762, (M+1)⁺.

ELEM ANAL CALCD: C, 74.85%; H, 5.17%; N, 2.57%. Found: C, 74.53%; H, 5.43%, 2.49%. ¹H-NMR (ppm, DMSO-d₆), δ = 1.5 (CH₃), 4.6 (N-CH₂-ph), 5.4 (N-CH₂-O), 6.6–8.0 (Ar-H), 9.5 (OH).

Synthesis of (4)

Exactly 2.73 g (0.005 mol) of (**3**), 0.892 g (0.006 mol) of potassium carbonate, 0.892 g (0.006 mol) of propargyl bromide, and 30 mL of acetone were introduced into a 100 mL round-bottom glass flask equipped with a condenser and a magnetic stirrer. The mixture was stirred at reflux for 24 h. After that, the mixture was filtered (to remove KBr) and the filtrate was poured into DI water. The precipitate was filtered and dried (60% yield). An exothermic peak at 252 °C with enthalpy of 319 J/g was observed in the DSC thermogram. HR-MS(FAB+) *m/z*: calcd. for C₃₇H₃₀O₄NP 583.1912; anal., 584.1919, (M+1)⁺.

ELEM ANAL CALCD: C, 76.15%; H, 5.18%; N, 2.40%. Found: C, 74.83%; H, 5.83%, 2.18%. ¹H-NMR (ppm, DMSO-d₆), δ = 1.8 (CH₃), 2.5 (HC≡C-), 4.5 (O-CH₂-ph), 4.6 (C≡C-CH₂-O), 5.3 (N-CH₂-O), 6.6–8.0 (Ar-H).

Preparation of the Epoxy Thermosets

The epoxy thermosets were obtained via the thermal curing of (**3**) and (**4**) with commercially-available epoxy resins: DGEBA and CNE. The curing agent and epoxy with 1/1 equivalent ratio were mixed and stirred homogeneously in an aluminum mold at 140 °C, and then cumulatively cured at 160, 200 and 220 °C for 2 h each in an air-circulating

oven. Three types of samples were prepared: $12.7 \times 1.27 \times 0.127 \text{ cm}^3$ for UL-94 measurement, $5.0 \times 1.0 \times 0.2 \text{ cm}^3$ for DMA measurement and $1.0 \times 1.0 \times 0.2 \text{ cm}^3$ for TMA, dielectric and water absorption measurements. The sample IDs for (3)-cured DGEBA and CNE are named (3)/DGEBA and (3)/CNE, respectively. The sample IDs for (4)-cured DGEBA and CNE are named (4)/DGEBA and (4)/CNE, respectively.

Characterization

Differential scanning calorimetry (DSC) was performed with a Perkin-Elmer DSC 7 in a nitrogen atmosphere at a heating rate of $10 \text{ min}/^\circ\text{C}$. Thermal gravimetric analysis (TGA) was performed with a Perkin-Elmer Pyris1 at a heating rate of $20 \text{ }^\circ\text{C}/\text{min}$ in a nitrogen atmosphere. Dynamic mechanical analysis (DMA) was performed with a Perkin-Elmer Pyris Diamond DMA with a sample size of $5.0 \times 1.0 \times 0.2 \text{ cm}^3$. The storage modulus E' and $\tan \delta$ were determined as the sample was subjected to the temperature scan mode at a programmed heating rate of $5 \text{ }^\circ\text{C}/\text{min}$ at a frequency of 1 Hz. The test was performed by a bending mode with an amplitude of $5 \text{ }\mu\text{m}$. Thermal mechanical analysis (TMA) was performed with a Perkin-Elmer Pyris Diamond TMA at a heating rate of $5 \text{ }^\circ\text{C}/\text{min}$ with a sample size of $1.0 \times 1.0 \times 0.2 \text{ cm}^3$ in a penetration mode. NMR measurements were performed using a Varian Inova 600 NMR in $\text{DMSO-}d_6$, and the chemical shift was calibrated by setting the chemical shift of $\text{DMSO-}d_6$ as 2.49 ppm. IR spectra were measured by a Perkin-Elmer RX1 infrared spectrophotometer in KBr powder form. High resolution mass spectra were obtained by a Finnigan/Thermo Quest MAT 95XL mass spectrometer. The UL-94 vertical test was performed according to the testing procedure of FMVSS 302/ZSO 3975 with a test specimen bar of 127 mm in length, 12.7 mm in width and about 1.27 mm in thickness. The height of the burner flame was 25 mm and the height from the top of the burner to the bottom of the test bar was 10 mm. During the test, the polymer specimen

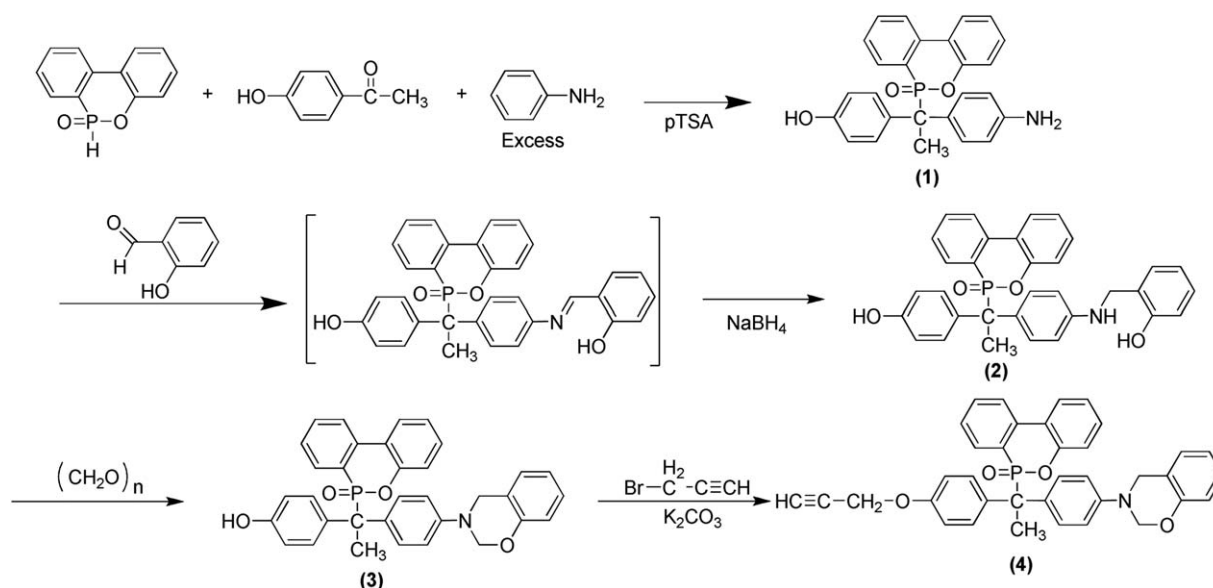
was subjected to two 10-s ignitions. After the first ignition, the flame was removed and the time for the polymer to self-extinguish (t_1) was recorded. Cotton ignition was noted if polymer dripping occurred during the test. After cooling, the second ignition was performed on the same sample. The self-extinguishing time (t_2) and dripping characteristics were again recorded. Five specimens were measured and the average burning time was recorded. If t_1 plus t_2 was less than 10 s with no dripping, it was considered to be a V-0 grade, an industrial standard for flame-retardancy. If t_1 plus t_2 was in the range of 10 to 30 s without any dripping, the polymer was considered to be a V-1 material. If t_1 plus t_2 was in the range of 10 to 30 s with dripping that ignited a cotton indicator located below the sample, the polymer was considered to be a V-2 material.

RESULTS AND DISCUSSION

Synthesis and Characterization of (4)

A propargyl ether-containing benzoxazine (4) was prepared from the nucleophilic substitution of a phenolic OH-containing benzoxazine (3) with propargyl bromide in the presence of potassium carbonate (Scheme 1). The precursor (3) was prepared from the condensation of (1) with 2-hydroxybenzaldehyde, followed by the reduction of the imine linkage by NaBH_4 , and ring closure condensation of (2) with formaldehyde.

Supporting Information Figure S1 shows the $^1\text{H-NMR}$ spectra of (2). The disappearance of the amino signal of (1) at 5.0 ppm, and the appearance of the methylene signal at 4.2 ppm and secondary amine signal at 6.0 ppm support the successful preparation of (2). Figure 1 shows the $^1\text{H-NMR}$ spectra of (3-4). The disappearance of the phenolic OH signal of (3) and the appearance of propargyl ether peaks at 2.5 (H^b) and 4.6 (H^c) ppm support the transformation of phenolic OH to



SCHEME 1 Synthesis of benzoxazine (4).

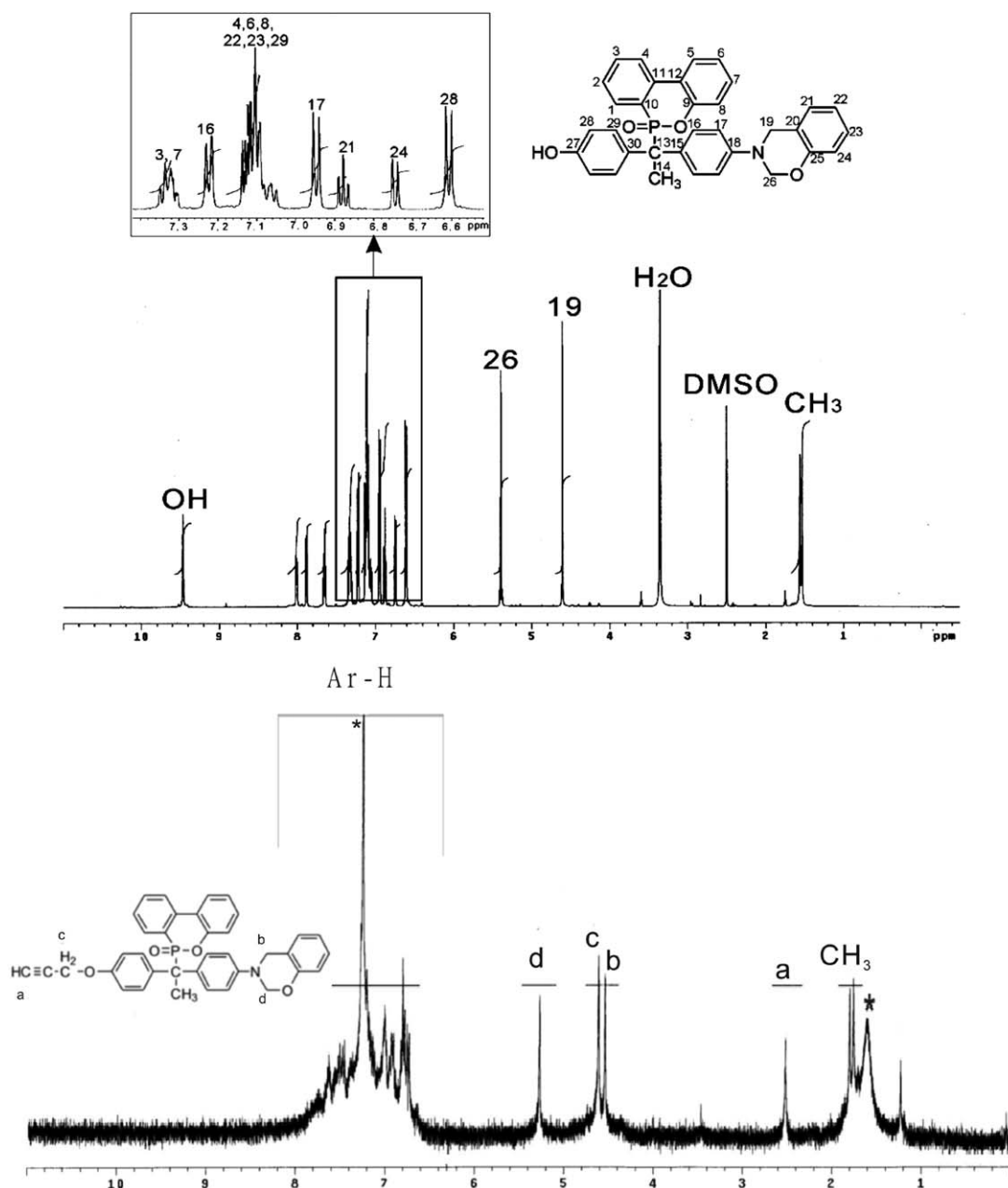


FIGURE 1 $^1\text{H-NMR}$ spectrum of (3) and (4).

propargyl ether. In addition, the oxazine signals at 4.5 (H^c) and 5.3 (H^d) ppm indicates the stability of the oxazine linkage in this potassium carbonate-catalyzed reaction.

DSC Thermograms

Figure 2 shows the DSC thermograms of (3), (4), and (4'), which was prepared from the Mannich condensation of 1,1-bis(4-aminophenyl)-1-(6-oxido-6H-dibenz <c,e> <1,2> oxaphosphorin-6-yl)ethane, paraformaldehyde, and phenol.³³ A melting point at 239 °C and a rapid exothermic peak at 244 °C were observed for (3). The rapid exotherm after melting indicates (3) is difficult to process. For (4), an exotherm with two peaks at 252 °C and 270 °C, respectively, were observed. The total enthalpy of the exothermic peak is as

high as 319 J/g, which is much higher than that (134 J/g) of analogous benzoxazine (4'), which is a difunctional phosphinated benzoxazine without the propargyl ether linkage. Compared with the peak patterns of (4) and (4'), we proposed that the second exothermic peak of (4) is related to the curing propargyl ether linkage. The curing of (4) was monitored by IR spectra and discussed below to prove the proposal.

Microstructure

Figure 3 shows the IR spectra of (4) after accumulative curing. The curing temperature and curing time are marked in Figure 3. The characteristic absorptions of benzene with an attached oxazine ring at 975 cm^{-1} , oxazine at 1376 and 1032 cm^{-1} , and propargyl ether at 2120 cm^{-1} decreased

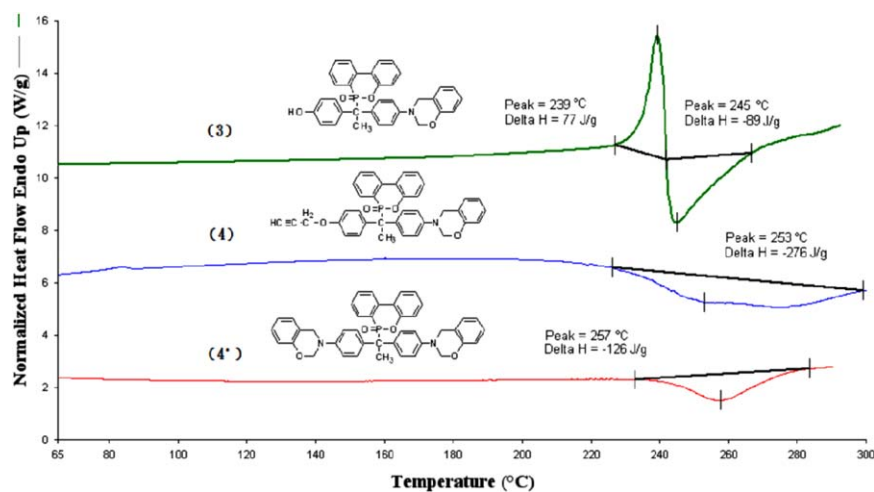


FIGURE 2 DSC thermograms of **(3)**, **(4)** and **(4')**. [Color figure can be viewed in the online issue, which is available at wileyonlinelibrary.com.]

gradually with the progress of curing. A C=C absorption of benzopyran at 1680 cm^{-1} , which resulted from the Claisen type rearrangement of propargyl ether, appeared after curing at $180\text{ }^{\circ}\text{C}$, but decreased gradually with the progress of curing, and disappeared after curing at $240\text{ }^{\circ}\text{C}$. Figure 4 shows the DSC thermogram of **(4)** after accumulative curing (the same thermal history as in Fig. 3). The first exothermic enthalpy decreased obviously with the progress of curing. IR and DSC data suggest that the ring opening of oxazine and the formation of benzopyran are correlated with the first DSC exotherm. The second exothermic peak decreased obviously after curing at $220\text{ }^{\circ}\text{C}$, and disappeared after curing at $240\text{ }^{\circ}\text{C}$. From IR and DSC data, the second exotherm is related to the polymerization of the C=C bond of benzopyran. According to the data in Figures 3 and 4, a two-stage

polymerization mechanism of **(4)** was proposed in Scheme 2. This first stage is related to the ring opening of the oxazine and Claisen type rearrangement of propargyl ether, and the second stage is the polymerization of the C=C bond of benzopyran. This observation is consistent with data reported in previous studies.^{19–26}

Properties of Epoxy Thermosets

We initially used **(1)**, **(3)** and **(4)** as epoxy curing agents. However, the melting point of **(1)** was as high as $294\text{ }^{\circ}\text{C}$ (Supporting Information Fig. S2), hindering the processing and preparation of the epoxy thermoset. Supporting Information Figure S3 shows the DSC thermograms of powder mixtures of **(3)**/DGEBA and **(4)**/DGEBA. The onset exothermic temperature of **(3)**/DGEBA starts at $160\text{ }^{\circ}\text{C}$, which is much lower than self-curing of **(3)**. The nucleophilic addition of phenolic OH of **(3)** on epoxy resin is thought to be responsible for the exothermic peak. However, the exothermic enthalpy is not high. We speculate that the melting enthalpy of **(3)**, which is $239\text{ }^{\circ}\text{C}$ as shown in Figure 2, compensates the exothermic peak. The onset exothermic temperature of **(4)**/DGEBA is similar to that of **(4)**. If some ring-opened structures exist in **(4)**, the onset exothermic temperature will reduce remarkably. This result indicates that no or little ring-opened structures exist in **(4)**, supporting the purity of **(4)**. Figure 5 shows DMA thermograms of the resulting epoxy thermosets. The T_g value of the **(4)**/CNE is $227\text{ }^{\circ}\text{C}$, which is $31\text{ }^{\circ}\text{C}$ higher than that of the **(3)**/CNE. A similar trend was observed for **(3)**/DGEBA and **(4)**/DGEBA (Table 1). Moreover, as shown in Figure (5 and 3)-cured thermosets display higher modulus than 4-cured thermosets. It is thought that the modulus is strongly related with the intermolecular interaction. The 3-cured thermoset exhibits more second alcohol for intermolecular interaction. In addition, the 4-cured thermosets exhibits higher free volume due to the double-strain structure (Scheme 3, to be discussed later). Figure 6 shows the TMA thermograms of the resulting epoxy thermosets. The T_g value defined by TMA is $212\text{ }^{\circ}\text{C}$ for **(4)**/CNE, which is $45\text{ }^{\circ}\text{C}$ higher than that of **(3)**/CNE. The

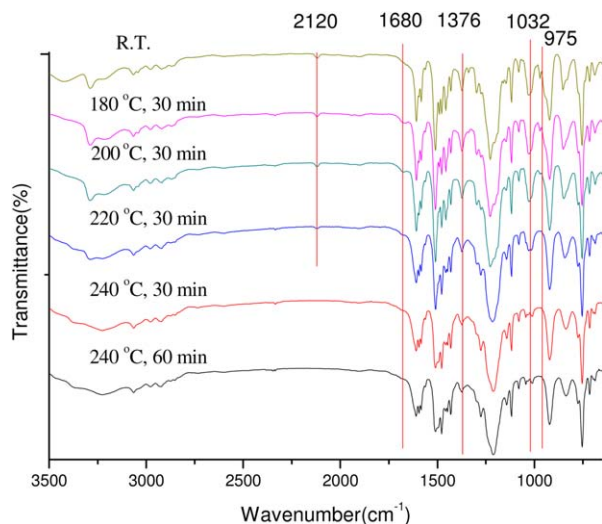


FIGURE 3 IR spectra **(4)** after accumulative curing. The curing temperature and curing time are marked in the Figure. [Color figure can be viewed in the online issue, which is available at wileyonlinelibrary.com.]

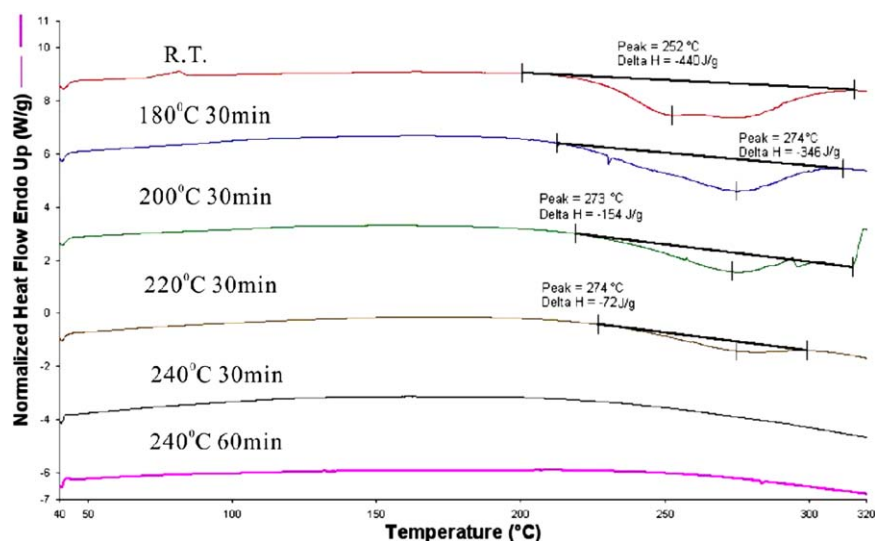
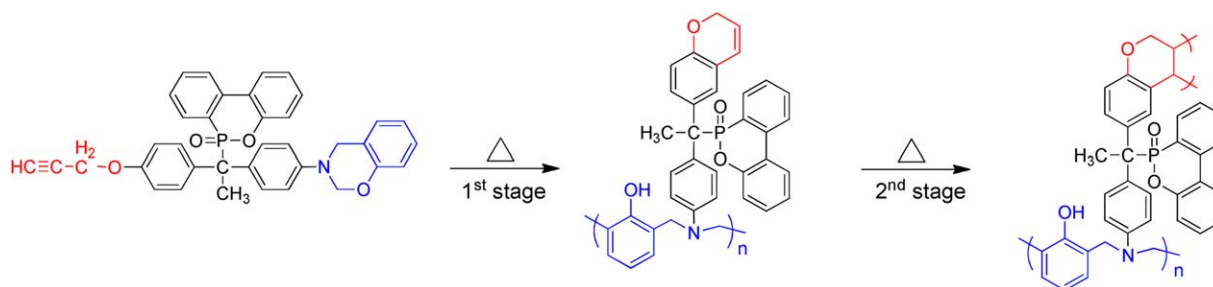


FIGURE 4 DSC thermograms of **(4)** after accumulative curing (the same thermal history as in Fig. 3). [Color figure can be viewed in the online issue, which is available at wileyonlinelibrary.com.]



SCHEME 2 Proposed polymerization mechanism of **(4)**. [Color figure can be viewed in the online issue, which is available at wileyonlinelibrary.com.]

coefficient of thermal expansion (CTE) of **(4)**/CNE is 47 ppm/°C, which is smaller than that (56 ppm/°C) of **(3)**/CNE. A similar trend was observed for **(3)**/DGEBA and **(4)**/DGEBA (Table 1). The 5 wt % degradation temperature is 393 °C for **(4)**/CNE, while the value reduces to 348 °C for

(3)/CNE (Fig. 7). The char yield also reduces from 40 for **(4)**/CNE to 33 for **(3)**/CNE. A similar result was observed for **(3)**/DGEBA and **(4)**/DGEBA (Table 1). DMA, TMA and TGA data demonstrate the advantage of the propargyl ether linkage in thermal properties over phenolic OH as an epoxy curing agent. Table 1 also lists the UL-94 result of the resulting epoxy thermosets. UL-94 V-0 grade can be achieved for all systems. This result demonstrates the good flame retardancy of the phosphinate pendant.

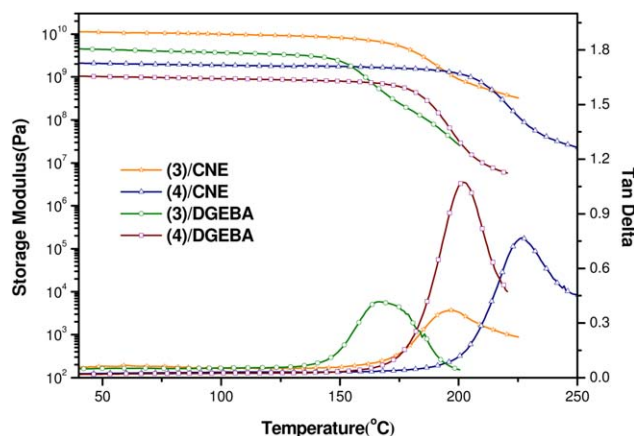


FIGURE 5 DMA thermograms of the resulting epoxy thermosets. [Color figure can be viewed in the online issue, which is available at wileyonlinelibrary.com.]

Dielectric Properties

The advantage of propargyl ether in the dielectric constant (D_k) and dissipation factor (D_f) can be supported by the dielectric values of the epoxy thermosets (Table 2). D_k and D_f of **(4)**/CNE at 1 GHz are 2.62 U and 4.6 mU, respectively, which are much lower than those (3.60 U and 26.7 mU) of **(3)**/CNE. A similar trend was observed for **(3)**/DGEBA and **(4)**/DGEBA (Table 2). Hougham et al.^{16,17} reported that the dielectric constant could be reduced by increasing molecule's hydrophobicity, free volume, and by decreasing polarization. According to the data shown in Figures 2 to 4, the curing of the benzopyran leads to a low-polar aliphatic cycloether structure (Scheme 3), which can result in a low-dielectric

TABLE 1 Thermal Properties of the Resulting Epoxy Thermosets

Thermoset ID	T_g ($^{\circ}\text{C}$) ^a	T_g ($^{\circ}\text{C}$) ^b	CTE (ppm/ $^{\circ}\text{C}$) ^c	$T_{d5\%}$ ($^{\circ}\text{C}$) ^d	Char yield (wt %) ^e	Dripping	UL-94 Grade
(3)/DGEBA	173	159	56	341	27	No	V-0
(4)/DGEBA	202	190	47	388	33	No	V-0
(3)/CNE	196	167	56	348	33	No	V-0
(4)/CNE	227	212	47	393	40	No	V-0

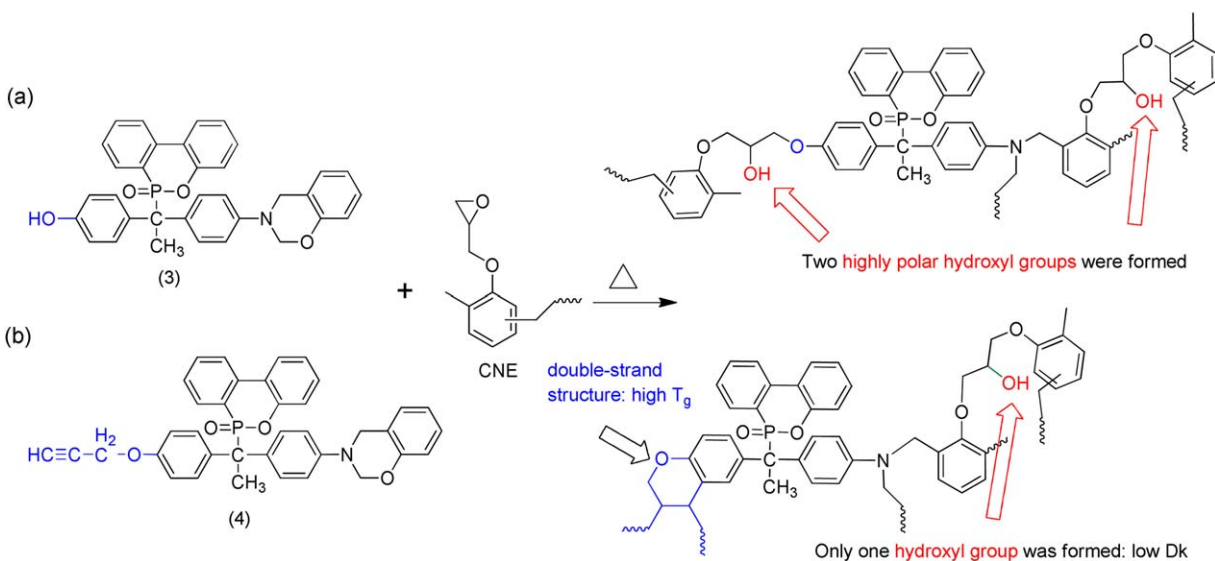
^a Peak temperature of tan(delta) measured by DMA at a heating rate of 5 $^{\circ}\text{C}/\text{min}$.

^b Measured by TMA at a heating rate of 5 $^{\circ}\text{C}/\text{min}$.

^c Coefficient of thermal expansion are recorded from 50 $^{\circ}\text{C}$ to 150 $^{\circ}\text{C}$.

^d Temperature corresponding to 5% weight loss by thermogravimetry at a heating rate of 20 $^{\circ}\text{C}/\text{min}$ in the atmosphere of nitrogen.

^e Residual weight % at 800 $^{\circ}\text{C}$ in the atmosphere of nitrogen.



SCHEME 3 Proposed structure of the (a) (3)/CNE and (b) (4)/CNE thermosets. [Color figure can be viewed in the online issue, which is available at wileyonlinelibrary.com.]

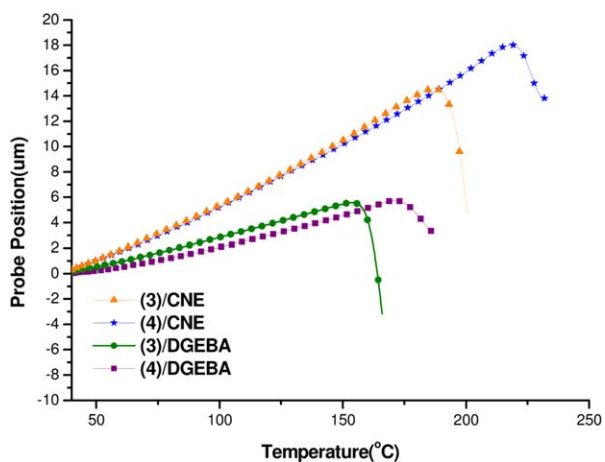


FIGURE 6 TMA thermograms of the resulting epoxy thermosets. [Color figure can be viewed in the online issue, which is available at wileyonlinelibrary.com.]

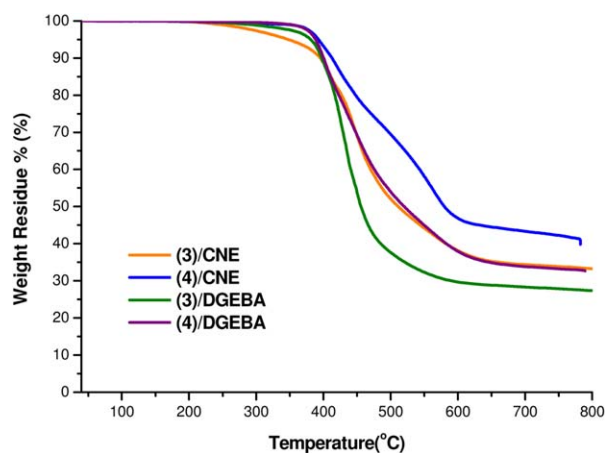


FIGURE 7 TGA thermograms of the resulting epoxy thermosets. [Color figure can be viewed in the online issue, which is available at wileyonlinelibrary.com.]

TABLE 2 Dielectric Properties and Water Absorption of the Resulting Epoxy Thermosets

Thermoset ID	D_k (U)		D_f (mU)		Water Absorption at 100 °C (25 °C) ^a		
	1 GHz	100 MHz	1 GHz	100 MHz	12 h	24 h	48 h
(3) /DGEBA	3.32 ± 0.01	3.43 ± 0.02	17.57 ± 0.02	20.66 ± 0.03	2.22(0.50)	2.38(0.74)	3.10(1.12)
(4) /DGEBA	2.77 ± 0.01	2.81 ± 0.02	6.76 ± 0.01	6.94 ± 0.02	0.27(0.12)	1.31(0.25)	1.95(0.37)
(3) /CNE	3.60 ± 0.01	3.79 ± 0.02	26.73 ± 0.02	30.55 ± 0.03	3.14(0.86)	3.47(1.60)	3.63(1.84)
(4) /CNE	2.62 ± 0.01	2.65 ± 0.01	4.62 ± 0.01	5.27 ± 0.02	1.04(0.54)	1.73(0.72)	2.79(1.26)

^a The value in parentheses is the water absorption at 25 °C.

value. In addition, the bulky cycloether structure that increases the free volume of the thermoset might also be responsible for the low D_k and D_f . Particularly, as shown in Scheme 3(a), two secondary alcohols were formed for each **(3)** curing with epoxy. However, as shown in Scheme 3(b), only one secondary alcohol was formed for each **(4)** curing with epoxy. It is known that secondary alcohol in the epoxy thermosets is a highly polar linkage that leads to increased D_k and D_f . Therefore, the formation of aliphatic cycloether and half amounts of secondary alcohol in the **(4)**-cured epoxy thermoset are thought to partially be responsible for the lower dielectric D_k and D_f . It is known that aryl esterized phenol compounds, active esters, have been used as epoxy curing agents to eliminate the formation of secondary alcohol.^{34,35} However, thermosets cured by active esters usually display a lower T_g than those cured by their phenol precursors. In this case, an enhancement in T_g and reduction in dielectric properties was simultaneously achieved, which is rarely seen in the literature. Table 2 lists the water absorption of the resulting epoxy thermosets. **(4)**/CNE and **(4)**/DGEBA display much lower absorption values than **(3)**/CNE and **(3)**/DGEBA, no matter at 100 °C or at 25 °C. The trend is consistent with that of the dielectric properties. The formation of half amounts of highly polar secondary alcohol is thought to be responsible for the result.

CONCLUSIONS

We have successfully prepared a propargyl ether-containing benzoxazine **(4)** by a four-step procedure from **(1)**. According to the IR and DSC data, a two-stage polymerization mechanism was proposed: the first stage is related to the ring opening of the oxazine and Claisen rearrangement of propargyl ether; and the second stage is the polymerization of the C=C bond of benzopyran. Epoxy thermosets cured by **(4)** display better properties than those cured by **(3)** in T_g , dimensional stability, thermal stability, dielectric properties, and water absorption. In particular, thermosets cured by **(4)** show low-dielectric characteristic, which should be attractive for application in high-frequency printed circuit boards. We proposed that the formation of aliphatic cycloether and half the amount of secondary alcohol in the **(4)**-cured epoxy thermoset are responsible for the lower dielectric D_k and D_f . The high- T_g characteristic of propargyl ether-containing has been reported in the literature; however, to the best of our knowledge, this is the first article reporting the low-dielectric characteristic of propargyl ether-containing benzoxazines as epoxy curing agents.

ACKNOWLEDGMENTS

The authors thank the National Science Council of the Republic of China for financial support. Partial sponsorship by the Green Chemistry Project (NCHU), as funded by the Ministry of Education, is also gratefully acknowledged.

REFERENCES AND NOTES

- X. Ning, H. Ishida, *J. Polym. Sci. Part A: Polym. Chem.* **1994**, *32*, 1121–1129.
- Y. Yagci, B. Kiskan, N. N. Ghosh, *J. Polym. Sci. Part A: Polym. Chem.* **2009**, *47*, 5565–5576.
- I. Hamerton, B. J. Howlin, A. L. Mitchell, L. T. McNamara, S. Takeda, *React. Funct. Polym.* **2012**, *72*, 736–744.
- Y.-C. Su, F.-C. Chang, *Polymer* **2003**, *44*, 7989–7996.
- C. H. Lin, S. L. Chang, H. H. Lee, H. C. Chang, K. Y. Hwang, A. P. Tu, W. C. Su, *J. Polym. Sci. Part A: Polym. Chem.* **2008**, *46*, 4970–4983.
- P. Velez-Herrera, K. Doyama, H. Abe, H. Ishida, *Macromolecules* **2008**, *41*, 9704–9714.
- M. R. Vengatesan, S. Devaraju, A. A. Kumar, M. Alagar, *High Perform. Polym.* **2011**, *23*, 441–456.
- Y.-J. Lee, J.-M. Huang, S.-W. Kuo, J.-K. Chen, F.-C. Chang, *Polymer* **2005**, *46*, 2320–2330.
- Y.-J. Lee, S.-W. Kuo, C.-F. Huang, F.-C. Chang, *Polymer* **2006**, *47*, 4378–4386.
- Y.-J. Lee, S.-W. Kuo, Y.-C. Su, J.-K. Chen, C.-W. Tu, F.-C. Chang, *Polymer* **2004**, *45*, 6321–6331.
- M.-C. Tseng, Y.-L. Liu, *Polymer* **2010**, *51*, 5567–5575.
- Y.-C. Su, W.-C. Chen, K.-L. Ou, F.-C. Chang, *Polymer* **2005**, *46*, 3758–3766.
- J.-Y. Shieh, C.-Y.; Lin, C.-L. Huang, C.-S. Wang, *J. Appl. Polym. Sci.* **2006**, *101*, 342–347.
- P. Yang, Y. Gu, *J. Appl. Polym. Sci.* **2012**, *124*, 2415–2422.
- K. Zhang, Q. Zhuang, Y. Zhou, X. Liu, G. Yang, Z. Han, *J. Polym. Sci. Part A: Polym. Chem.* **2012**, *50*, 5115–5123.
- G. Hougham, G. Tesoro, J. Shaw, The synthesis and properties of polyimides made from perfluoro aromatic diamines. *Polym. Mater. Sci. Eng.* **1989**, *61*, 369.
- G. Hougham, G. Tesoro, J. Shaw, *Macromolecules* **1994**, *27*, 3642–3649.
- H. C. Chang, H. T. Lin, C. H. Lin, *Polym. Chem.* **2012**, *3*, 970–978.
- M. F. Grenier-Loustalot, V. Denizot, D. Beziere, *High Perform. Polym.* **1995**, *7*, 157–180.
- M. F. Genier-Loustalot, C. Sanglar, *High Perform. Polym.* **1996**, *8*, 315–339.

- 21** M. F. Grenier-Loustalot, C. Sanglar, *High Perform. Polym.* **1996**, *8*, 341–361.
- 22** M. F. Grenier-Loustalot, C. Sanglar, *High Perform. Polym.* **1996**, *8*, 533–554.
- 23** M. F. Grenier-Loustalot, C. Sanglar, *High Perform. Polym.* **1996**, *8*, 555–578.
- 24** W. E. Douglas, A. S. Overend, *Eur. Polym. J.* **1991**, *27*, 1279–1287.
- 25** C. P. R. Nair, R. L. Bindu, K. Krishnan, K. N. Ninan, *Eur. Polym. J.* **1999**, *35*, 235–246.
- 26** S. Prieto, M. Galia, V. Cadiz, *Macromol. Chem. Phys.* **1998**, *199*, 1291–1300.
- 27** T. Agag, T. Takeichi, *Macromolecules* **2001**, *34*, 7257–7263.
- 28** B. Kiskan, G. Demiray, Y. Yagci, *J. Polym. Sci. Part A: Polym. Chem.* **2008**, *46*, 3512–3518.
- 29** A. Chernykh, T. Agag, H. Ishida, *Polymer* **2009**, *50*, 382–390.
- 30** A. Chernykh, T. Agag, H. Ishida, *Macromolecules* **2009**, *42*, 5121–5127.
- 31** H. C. Chang, C. H. Lin, H. T. Lin, S. A. Dai, *J. Polym. Sci. Part A: Polym. Chem.* **2012**, *50*, 1008–1017.
- 32** C. H. Lin, S. L. Chang, P. W. Cheng, *J. Polym. Sci. Part A: Polym. Chem.* **2011**, *49*, 1331–1340.
- 33** C. H. Lin, unpublished work.
- 34** T. Kan, S. Etsuko, M. Kunihiro, A. Kazuo, Active ester resin, method for producing same, thermosetting resin composition, cured product thereof, semiconductor sealing material, prepreg, circuit board, and build-up film. **2012**.
- 35** A. Kazuo, S. Etsuko, Thermosetting resin composition, cured product thereof, active ester resin, semiconductor sealing material, prepreg, printed circuit board, and build-up film. **2012**.